Cerebral Cortex, February 2018;28: 791–804

doi: 10.1093/cercor/bhx331
Advance Access Publication Date: 1 December 2017
Original Article

ORIGINAL ARTICLE

Distal Functional Connectivity of Known and Emerging Cortical Targets for Therapeutic Noninvasive Stimulation

Nuria Doñamayor[1], Kwangyeol Baek[1,2,3] and Valerie Voon[1,4,5,6]

[1]Department of Psychiatry, University of Cambridge, Cambridge CB2 2QQ, UK, [2]Athinoula A. Martinos Center for Biomedical Imaging, Massachusetts General Hospital, Charlestown, MA 02129, USA, [3]Department of Radiology, Harvard Medical School, Boston, MA 02115, USA, [4]Behavioural and Clinical Neurosciences Institute, University of Cambridge, Cambridge CB2 3EB, UK, [5]Cambridgeshire and Peterborough NHS Foundation Trust, Cambridge CB21 5EF, UK and [6]NIHR Cambridge Biomedical Research Centre, Cambridge CB2 0QQ, UK

Address correspondence to Valerie Voon, Department of Psychiatry, University of Cambridge, Addenbrooke's Hospital, Level E4, Box 189, Cambridge CB2 0QQ, UK. Email: vv247@cam.ac.uk.

Abstract

Noninvasive stimulation is an emerging modality for the treatment of psychiatric disorders, including addiction. A crucial element in effective cortical target selection is its distal influence. We approached this question by examining resting-state functional connectivity patterns in known and potential stimulation targets in 145 healthy adults. We compared connectivity patterns with distant regions of particular relevance in the development and maintenance of addiction. We used stringent Bonferroni-correction for multiple comparisons. We show how the anterior insula, dorsal anterior cingulate, and ventromedial prefrontal cortex had opposing functional connectivity with striatum compared to the dorsomedial prefrontal cortex. However, the dorsolateral prefrontal cortex, the currently preferred target, and the presupplementary motor area had strongest negative connections to amygdala and hippocampus. Our findings highlight differential and opposing influences as a function of cortical site, underscoring the relevance of careful cortical target selection dependent on the desired effect on subcortical structures. We show the relevance of dorsal anterior cingulate and ventromedial prefrontal cortex as emerging cortical targets, and further emphasize the anterior insula as a potential promising target in addiction treatment, given its strong connections to ventral striatum, putamen, and substantia nigra.

Key words: addiction, anterior insula, prefrontal cortex, resting-state functional connectivity, transcranial magnetic stimulation

Introduction

The use of noninvasive stimulation, such as repetitive transcranial magnetic stimulation (rTMS) or transcranial direct current stimulation (tDCS), to treat psychiatric disorders is an emerging field (Post and Keck 2001; Gorelick et al. 2014). High-frequency rTMS increases cortical excitability, blood flow, and metabolism, while low-frequency stimulation has a net inhibitory effect (Post and Keck 2001). Similarly, anodal tDCS enhances cortical excitability and cathodal stimulation diminishes excitability (Nitsche and Paulus 2000), although the effects of cathodal stimulation on cognitive function have been inconsistent (Jacobson et al. 2012). A number of studies have demonstrated that both rTMS

and tDCS of different cortical regions provoke changes in resting-state functional connectivity networks (for reviews see Fox, Halko, et al. 2012; Saiote et al. 2013). rTMS targeting the dorsolateral prefrontal cortex (dlPFC) for major depression has been shown to be safe and effective (Noda et al. 2015), but the target sites for disorders of addiction remain to be established. Understanding influences on distal subcortical structures, that is, deeper regions which are beyond the direct effects of superficial noninvasive stimulation and likely related to its secondary downstream effects, is critical to target selection.

To date, most addiction research has focused on dlPFC stimulation for the treatment of alcohol dependence (Mishra et al. 2010; Klauss et al. 2014) and other substance addictions (Eichhammer et al. 2003; Camprodon et al. 2007; Li et al. 2013), with promising but mixed results. High-frequency rTMS of the right dlPFC at 10 Hz has been shown to reduce craving (Mishra et al. 2010), but not stimulation of the left side at 20 Hz (Höppner et al. 2011). Interestingly, anodal tDCS of the left dlPFC has been found to reduce alcohol craving (da Silva et al. 2013), but simultaneous anodal and cathodal stimulation of the right and left dlPFC, respectively, has shown no effect (Klauss et al. 2014). However, 2 recent studies (Rapinesi et al. 2013; Girardi et al. 2015) with bilateral high-frequency deep rTMS of the dlPFC reported significant reduction in craving and dysthymic symptoms. Results from studies in cocaine use disorder targeting the dlPFC have been equally mixed (Camprodon et al. 2007; Politi et al. 2008; Gorini et al. 2014; Terraneo et al. 2016). Given these disparate results, finding new potential targets is critical.

Emerging targets for addictions include midline prefrontal targets. Low- and high- frequency deep rTMS of dorsal anterior cingulate cortex (ACC) and dorsomedial PFC (dmPFC), respectively, were recently shown to reduce craving in alcohol dependence (De Ridder et al. 2011; Ceccanti et al. 2015). High-frequency dmPFC simulation additionally decreased the mean number of alcoholic drinks taken (Ceccanti et al. 2015). There is also been increasing interest in targeting the ventromedial PFC (vmPFC), which is thought to be part of the network mediating abnormal incentive salience of drug cues compared to natural reinforcers (Koob and Volkow 2010). Low-frequency TMS of the frontal pole/vmPFC has been shown to be more likely to attenuate cocaine craving than sham TMS, as well as to decrease activity in the striatum and anterior insula (Hanlon et al. 2015). Others have attempted to target the vmPFC through tDCS stimulation of the dlPFC: simultaneous anodal and cathodal stimulation of the right and left dlPFC, respectively, in crack cocaine users was followed by increased diffusion tensor parameters in the tract connecting vmPFC and nucleus accumbens (NAcc), which further correlated with a decrease in craving (Nakamura-Palacios et al. 2016).

Anodal tDCS of the right inferior frontal cortex (IFC) in alcohol dependent subjects showed no effects (den Uyl et al. 2015), although this structure is essential in response inhibition (Cai, Ryali, et al. 2014), and anodal tDCS to this region has been shown to decrease impulsive behavior in healthy participants (Jacobson et al. 2011). Although the presupplementary motor area (pre-SMA) has not received much attention in addiction treatment, it deserves consideration given its central role in obsessive-compulsive disorder (D'Urso et al. 2016) and response inhibition (Cai, Cannistraci, et al. 2014), with impaired stopping behavior following disruption of pre-SMA activity (Cai et al. 2012). In the context of obsessive-compulsive disorder, which has been associated with pre-SMA hyperfunction, cathodal tDCS has been reported to alleviate symptoms (D'Urso et al. 2016).

Converging lesion, imaging and cognitive studies in humans have implicated a further cortical structure as central to addictions: the anterior insula (AI). Recent rodent studies have specifically pinpointed the AI as the neurobiological gate between impulsive and compulsive behaviors (Belin-Rauscent et al. 2016). Stroke lesions of the AI have been associated with cessation of smoking behavior and craving (Naqvi et al. 2007; Abdolahi et al. 2015). Similarly, deep high-frequency rTMS targeting AI and lateral PFC has shown reductions in nicotine consumption and quit rate maintained over 6 months (Dinur-Klein et al. 2014). Recent studies have further highlighted the importance of right AI connectivity for cue-induced craving (Moran-Santa Maria et al. 2015) and delay discounting (Clewett et al. 2014) in nicotine dependence. The AI has also been shown to play a critical role in cost-benefit decision making (Skvortsova et al. 2014), with increased activity in alcohol dependent participants when making decisions regarding drinking (MacKillop et al. 2014). Furthermore, reduced AI volume has been reported in alcohol dependent subjects (Makris et al. 2008; Senatorov et al. 2015), with this, as well as NAcc volume, increasing with alcohol abstinence (Makris et al. 2008).

Here, we used resting-state fMRI (rsfMRI) to investigate functional connectivity of potential and known rTMS and tDCS targets in a large sample of 145 healthy adults. Although functional brain organization has been shown to differ between addicted individuals and healthy controls (Gu et al. 2010; Ma et al. 2010; Janes et al. 2012; Sjoerds et al. 2017), resting-state functional connectivity in healthy subjects has proven useful in understanding the mechanisms of brain stimulation in pathology. A previous rsfMRI study reported that dlPFC TMS sites with better clinical efficacy in depression were more anticorrelated with the subgenual cingulate in healthy participants; a finding that was reproducible in patients with depression (Fox, Buckner, et al. 2012), demonstrating that rsfMRI data of healthy subjects could be used to optimize cortical target selection in a mental disorder. Further, another rsfMRI study on a healthy population seeded their analyses within deep brain stimulation targets for 14 disorders, including addiction, depression, epilepsy, Parkinson's disease, and obsessive-compulsive disorder, demonstrating that these structures were correlated with areas successfully used as inhibitory targets, and anticorrelated with cortical areas used as noninvasive excitatory targets (Fox et al. 2014).

We used a recently developed multiecho (ME) sequence and independent components analysis (ICA) shown to enhance signal-to-noise ratios 4-fold, hence, improving resolution of small subcortical structures (Kundu et al. 2012). We specifically compared the connectivity patterns of these cortical targets to relevant distal subcortical regions (striatal subregions, amygdala, hippocampus, and substantia nigra) known to play a key role in the development and maintenance of addiction. We contrasted connectivity between these cortical and distal areas using stringent Bonferroni-correction for multiple comparisons. These stimulation targets and distal regions are also highly relevant to other psychiatric disorders, such as obsessive-compulsive disorder. A fine-grained understanding of these corticosubcortical relationships may help in the selection of appropriate targets.

Materials and Methods

Participants

Data from 145 healthy volunteers (87 women, 27.52 ± 9.54 years old, range: 18–55) were used in this study. Participants were recruited from community and university-based advertisements

and were excluded if they had any current psychiatric (tested using the Mini International Neuropsychiatric Inventory) or neurological disorder, or were on psychotropic medication. Subjects were paid for their participation. Experimental procedures were approved by the University of Cambridge Research Ethics Committee and participants gave written informed consent.

rsfMRI Data Acquisition

rsfMRI data were acquired for 10 min while subjects fixated on a white cross on a black screen in a Siemens 3 T Tim Trio scanner using a 32-channel head coil at the Wolfson Brain Imaging Center, University of Cambridge. A ME EPI sequence was used with online reconstruction (TR = 2.47 s, FA = 78°, matrix size 64 × 64, 3.75 mm in-plane resolution, FOV = 240 mm, 32 oblique slices, alternating slice acquisition, slice thickness 3.75 mm with 10% gap, iPAT factor 3, bandwidth = 1698 Hz/pixel, TE = 12, 28, 44 and 60 ms). High-resolution anatomical images were acquired using a T1-weighted MPRAGE sequence (FOV = 176 × 240, 1 mm in-plane resolution, TI = 1100 ms).

rsfMRI Data Analysis

Data were analyzed with ME independent component analysis (ME-ICA; Kundu et al. 2012), which uses FastICA to decompose ME rsfMRI data, and the pseudo-*F*-statistics κ and ρ to categorize these as BOLD or non-BOLD activity, respectively. Nuisance regressors (low κ, high ρ) are then removed by projection. ME-ICA has been shown to enhance signal-to-noise ratios 4-fold, hence, improving resolution of small subcortical structures (Kundu et al. 2012) and being more sensitive to group differences than single-echo rsfMRI using conventional denoising techniques (Baek et al. 2017). Individual EPI images were then coregistered to the T1-weighted MPRAGE images and normalized to the MNI template. Data were spatially smoothed using a 6 mm FWHM Gaussian kernel and temporally band-pass filtered between 0.008 and 0.09 Hz. Anatomical images were segmented into grey and white matter and cerebrospinal fluid, and significant principal components of white matter and cerebrospinal fluid were removed. Seed-based functional connectivity analysis was performed with CONN-fMRI Functional Connectivity toolbox (Whitfield-Gabrieli and Nieto-Castañón 2012) for SPM8 (http://www.fil.ion.ucl.ac.uk/spm/software/spm8/), using bivariate correlation to measure the level of linear association between the time series of each seed and voxel. Seeds were manually created or altered using the MarsBaR region-of-interest (ROI) toolbox (Brett et al. 2002), as described previously (Morris et al. 2016). Age and gender were used as covariates of no interest.

Analyses were seeded within known and potential rTMS and tDCS target sites: left and right AI, bilateral dACC, left and right dlPFC, bilateral dmPFC, right IFC, bilateral pre-SMA, and bilateral vmPFC (see Supplementary Fig. S1). Medial targets were defined bilaterally, as differentiated unilateral stimulation of these regions is not always possible with the current methods. The AI seeds were defined by restraining the insula ROI from the automatic anatomical labeling (AAL) atlas at $y = 0$, retaining only the anterior portion. The dACC seed was defined by restricting the borders of the cingulate ROI from the AAL atlas at the tip and posterior end of the genu of the corpus callosum (CC) (Desikan et al. 2006; Cox et al. 2014). The dlPFC seeds were created by combining BA 9 and BA 46 from the AAL atlas, and restricting the anterior border by the most anterior tip of the CC, the posterior border by the genu of the CC, the ventral border by the inferior frontal sulcus and the medial border by the cingulate sulcus (Sanches et al. 2009; Cox et al. 2014). The dmPFC seed was created using area 10p (Öngür et al. 2003) as the anterior boundary, the lateral boundaries of the cingulate cortex as defined in the AAL atlas, and a vertical line through the genu of the CC as the posterior border. The right IFC seed was defined using the inferior frontal sulcus as the superior boundary, the precentral gyrus as the posterior boundary (Desikan et al. 2006; Cox et al. 2014) and the rostral extent of the inferior frontal sulcus as the anterior boundary (Desikan et al. 2006); which was then restricted using a 300 mm radius sphere centered on $x = \pm 48$, $y = 18$, $z = 8$ (Johnson-Frey et al. 2003) and with the anterior horizontal ramus of the Sylvian fissure as a boundary from orbital regions (Cox et al. 2014). The pre-SMA seed was defined by restraining the SMA ROI from the AAL atlas at the level of the anterior commisure (Kim et al. 2010), retaining only the anterior portion. The vmPFC seed was defined using area 10p (Öngür et al. 2003) as the anterior boundary, the cingulate cortex as lateral and posterior boundaries, the genu of the CC as the dorsal boundary, and $y = -18$ as the ventral boundary.

Six subcortical ROIs were further defined: ventral striatum (VS), caudate, putamen, amygdala, hippocampus and substantia nigra (SN) (see Supplementary Fig. S1). The VS ROI was created by Murray et al. (2007) based on the definition by Martinez et al. (2003). The caudate and putamen ROIs were based on the definitions by Martinez et al. (2003) and had no overlap with the VS ROI. Amygdala, hippocampus and SN ROIs were created from those defined in the Talairach Daemon atlas (Lancaster et al. 2000). All subcortical ROIs were defined bilaterally.

Seed-to-whole-brain connectivity maps were computed for each region and entered into a one-sample *t*-test, using a mask computed from the 6 subcortical ROIs (results of the seed-to-whole brain analysis without the subcortical mask can be found in Supplementary Information). Significant connectivity was identified using a threshold of $P < 0.006$ (whole-brain FWE-corrected) and a cluster threshold of $k \geq 5$. This threshold was selected by Bonferroni-correcting the standard $P < 0.05$ (FWE-corrected) threshold for the 9 seeds used.

Seed-to-ROI Connectivity

To compare seed-to-ROI connectivity strength between the cortical seeds used, individual subjects' Fisher z-transformed correlation coefficients averaged across the ROI were extracted for each ROI using the MarsBaR ROI toolbox (Brett et al. 2002).

The extracted Fisher z-transformed correlation coefficients were then inputted in a repeated-measures ANOVA (rmANOVA) for each of the 6 ROIs with the factor seed. Only seeds with significant connectivity to the ROI, as demonstrated by the preceding seed-to-whole brain analysis, were included in each rmANOVA. Huynh–Feldt-correction was used to correct degrees of freedom and *P*-values if Mauchly's sphericity test was significant. The *P*-values of the rmANOVAs were Bonferroni-corrected for 54 comparisons (9 seeds, 6 ROIs; e.g., the original *P*-value for the VS ROI was $P = 5.07e\text{-}93$, but here we report the Bonferroni-corrected *P*-value as $5.07e\text{-}93 \times 54 = 2.74e\text{-}91$). Post hoc *t*-tests were used to further examine the results of the significant rmANOVAs, and were Bonferroni-corrected for 9 seeds, 6 ROIs and the number of pairwise comparisons performed (e.g., $9 \times 6 \times 36 = 1944$ in the case of the VS, as all the seeds were inputted in the rmANOVA, but $9 \times 6 \times 15 = 810$ in the case of the hippocampus, since dmPFC, pre-SMA and vmPFC showed no significant connectivity to this ROI; the original *P*-value for the comparison between left AI and left dlPFC for the VS ROI was $P = 3.4e\text{-}14$, but here we report the Bonferroni-corrected *P*-value as $3.4e\text{-}14 \times 1944 = 6.61e\text{-}11$).

Results

Seed-to-Whole-Brain Connectivity

Seed-to-whole brain connectivity, masked with a network of interest comprising the 6 subcortical ROIs, was assessed for AI, dACC, dlPFC, dmPFC, right IFC, pre-SMA, and vmPFC seeds, which have been used or suggested as noninvasive stimulation targets (Fig. 1, Table 1). Results of the analysis without the subcortical mask can be seen in Figure 2.

Both left and right AI were functionally correlated with VS, caudate, and putamen, while showing a small cluster within the contralateral caudate that was anticorrelated with the seed. Further, the left AI was correlated with bilateral SN and ipsilateral amygdala, while the right AI showed the opposite pattern of correlation with ipsilateral SN and bilateral amygdala. Neither seed was significantly correlated with the hippocampus.

The dACC was significantly correlated with the VS and the anterior portions of the caudate and putamen, while the

Figure 1. Seed-to-whole brain resting-state functional connectivity of known and potential noninvasive stimulation targets. Results of the seed-to-whole brain resting-state functional connectivity masked with a network computed from the subcortical ROIs: striatum (VS is outlined in white), amygdala, hippocampus and SN. Images displayed at $P < 0.006$ (FWE-corrected) and $k > 0$.

Table 1 Results of the masked seed-to-whole-brain resting-state functional connectivity analyses performed on data from 145 healthy volunteers. Significant clusters were identified using a threshold of $P < 0.006$ (FWE-corrected) and $k \geq 5$. Plus (+) and minus (–) signs indicate the direction of the connectivity.

Seed	Peak region	x	y	z	k	t	P
Left AI (+)	L putamen	−27	12	7	692	30.00	<0.001
	L putamen	−27	12	−7		25.04	<0.001
	L putamen	−31	0	4		20.02	<0.001
	R putamen	31	12	4	665	25.26	<0.001
	R putamen	36	0	−3		16.66	<0.001
	R putamen	27	17	−7		15.85	<0.001
	L amygdala	−27	3	−19	40	13.82	<0.001
	L substantia nigra	−10	−18	−10	16	8.72	<0.001
	R substantia nigra	10	−16	−10	17	8.46	<0.001
Left AI (–)	R caudate	20	−2	23	6	4.95	0.001
Right AI (+)	R putamen	31	12	4	744	36.98	<0.001
	R putamen	36	0	−3		25.19	<0.001
	R putamen	27	17	−7		25.14	<0.001
	L putamen	−27	12	7	453	16.12	<0.001
	L putamen	−27	12	−7		14.46	<0.001
	L ventral striatum	−20	7	−12		11.88	<0.001
	R substantia nigra	10	−18	−10	18	11.77	<0.001
	L amygdala	−24	3	−19	8	8.04	<0.001
	R amygdala	27	3	−19	14	7.66	<0.001
Right AI (–)	L caudate	−6	14	9	19	5.43	<0.001
dACC (+)	R ventral striatum	15	17	−5	495	23.80	<0.001
	R putamen	27	17	−7		15.58	<0.001
	R putamen	29	14	7		9.79	<0.001
	L VS	−13	17	−5	398	21.63	<0.001
	L putamen	−27	12	7		6.40	<0.001
	R hippocampus	29	−37	−5	23	10.50	<0.001
	R hippocampus	29	−25	−12		8.66	<0.001
	L hippocampus	−27	−37	−5	14	9.90	<0.001
	L hippocampus	−29	−27	−12		6.62	<0.001
	L substantia nigra	−6	−14	−12	7	7.37	<0.001
	R substantia nigra	8	−11	−10	6	7.06	<0.001
dACC (–)	R amygdala	27	−4	−14	79	11.15	<0.001
	L amygdala	−24	−4	−19	92	10.83	<0.001
	L putamen	−31	−14	−7	20	6.77	<0.001
	L putamen	−27	−7	−7		5.94	<0.001
	L caudate	−17	−18	21	25	6.77	<0.001
	L caudate	−10	−4	16		6.08	<0.001
	R putamen	34	−2	7	47	5.70	<0.001
	R putamen	29	−14	4		5.35	<0.001
	R caudate	13	−9	18	5	5.64	<0.001
	L putamen	−29	−4	9	6	5.31	<0.001
	R putamen	29	−7	−7	5	5.22	<0.001
	R caudate	17	−18	21	7	5.11	0.001
Left dlPFC (+)	L caudate	−15	17	4	374	14.64	<0.001
	L putamen	−24	14	7		10.29	<0.001
	R caudate	20	19	7	146	10.58	<0.001
Left dlPFC (–)	R amygdala	22	−2	−14	151	12.99	<0.001
	R amygdala	29	0	−19		11.98	<0.001
	R hippocampus	29	−18	−14		9.78	<0.001
	L amygdala	−22	−4	−14	116	10.44	<0.001
	L hippocampus	−29	−14	−14		7.74	<0.001
	R substantia nigra	15	−20	−7	12	10.43	<0.001
	R putamen	34	−14	−7	65	9.18	<0.001
	R putamen	31	−18	2		5.75	<0.001
	R ventral striatum	6	10	−3	55	8.49	<0.001
	R caudate	10	0	11		4.89	0.001
	L ventral striatum	−3	12	−10	10	7.51	<0.001
	R putamen	34	−7	9	5	5.58	<0.001
Right dlPFC (+)	R putamen	29	17	2	322	14.05	<0.001
	R caudate	17	19	4		10.24	<0.001
	L caudate	−17	21	4	13	6.50	<0.001
	R putamen	34	5	−3	5	6.37	<0.001
Right dlPFC (–)	L amygdala	−20	−4	−14	157	13.29	<0.001
	L hippocampus	−29	−14	−14		10.44	<0.001
	L hippocampus	−29	−20	−10		9.72	<0.001
	L substantia nigra	−15	−20	−7	11	12.50	<0.001
	L ventral striatum	−3	10	−5	195	10.65	<0.001
	L caudate	−6	19	7		8.47	<0.001
	L caudate	−10	19	14		7.66	<0.001
	R amygdala	27	−4	−14	100	10.53	<0.001
	R hippocampus	29	−14	−14		6.39	<0.001
	L putamen	−31	−14	−7	57	10.43	<0.001
	R ventral striatum	6	10	−7	13	7.41	<0.001
	L putamen	−17	5	7	17	6.08	<0.001
dmPFC (+)	No suprathreshold clusters						
dmPFC (–)	L caudate	−15	24	0	442	12.67	<0.001
	L putamen	−27	14	2		8.96	<0.001
	L caudate	−3	14	7		6.92	<0.001
	L caudate	13	24	−3	401	11.78	<0.001
	R ventral striatum	17	12	−7		8.13	<0.001
	R ventral striatum	6	10	−3		7.28	<0.001
	L hippocampus	−29	−37	−3	6	7.89	<0.001
	R hippocampus	29	−39	0	7	6.32	<0.001
	R hippocampus	31	−34	−7		5.32	<0.001
	L caudate	−13	−4	21	41	6.25	<0.001
	L caudate	−17	12	21		5.40	<0.001
Right IFC (+)	R caudate	15	0	14	165	12.62	<0.001
	R putamen	20	5	7		8.17	<0.001
	R putamen	22	5	−3		5.80	<0.001
	R putamen	31	14	−3	160	12.18	<0.001
	R putamen	34	5	−3		11.65	<0.001
	R putamen	36	−11	−7		11.62	<0.001
	R substantia nigra	10	−18	−12	8	6.57	<0.001
	R amygdala	24	−2	−14	8	5.62	<0.001
Right IFC (–)	L ventral striatum	−10	21	−3	201	9.51	<0.001
	R caudate	20	26	2	71	8.64	<0.001
	R caudate	17	19	16		6.77	<0.001
pre-SMA (+)	L caudate	−15	10	11	348	17.05	<0.001
	L putamen	−20	3	4		10.27	<0.001
	L putamen	−22	19	−7		7.94	<0.001
	R caudate	17	12	9	236	15.03	<0.001
pre-SMA (–)	L hippocampus	−31	−34	−7	144	10.93	<0.001
	L hippocampus	−29	−27	−14		9.45	<0.001
	L amygdala	−22	−2	−17		9.17	<0.001
	R amygdala	22	−7	−21	159	10.45	<0.001
	R hippocampus	27	−14	−19		10.16	<0.001
	R hippocampus	31	−27	−14		10.15	<0.001
	R ventral striatum	6	10	−7	23	9.76	<0.001
	L ventral striatum	−3	12	−10	33	9.08	<0.001
	R putamen	36	−9	2	8	8.32	<0.001
	R putamen	34	−14	2	5	5.25	<0.001
vmPFC (+)	L hippocampus	−27	−37	−5	100	18.07	<0.001
	L hippocampus	−29	−18	−17		14.40	<0.001
	L hippocampus	−24	−9	−24		8.82	<0.001
	L ventral striatum	−3	10	−10	181	17.79	<0.001
	R ventral striatum	6	12	−7	170	16.85	<0.001
	R hippocampus	29	−34	−7	128	16.43	<0.001
	R hippocampus	29	−18	−17		16.39	<0.001
	R hippocampus	31	−27	−12		15.06	<0.001

Table 1 (Continued)

Seed	Peak region	x	y	z	k	t	P
vmPFC (–)	L caudate	−10	−2	16	278	11.10	<0.001
	L putamen	−22	−2	4		6.29	<0.001
	L putamen	−31	0	−3		5.12	<0.001
	R caudate	13	−4	16	95	8.02	<0.001
	R caudate	17	−18	21		5.17	<0.001
	R putamen	20	7	7	61	6.60	<0.001
	R putamen	34	5	0		6.48	<0.001

posterior portions showed small anticorrelated clusters. This seed was also correlated with bilateral SN as well as with posterior portions of the hippocampus, bilaterally. Furthermore, the dACC was significantly anticorrelated with bilateral amygdala.

Both left and right dlPFC were mostly positively associated with parts of the ipsilateral VS, as well as ipsilateral caudate and putamen, while showing mostly negative connections to portions of the contralateral structures. Both seeds were anticorrelated with bilateral amygdala and hippocampus, as well as with the contralateral SN.

The dmPFC was anticorrelated with bilateral VS, caudate and putamen, as well as with posterior portions of bilateral hippocampus. However, this region showed no significant correlations with amygdala or SN.

The right IFC was functionally correlated with ipsilateral caudate and putamen, but anticorrelated with the contralateral VS and caudate, as well as with anterior portions of the ipsilateral caudate. Further, this seed was positively associated with the ipsilateral amygdala and SN. However, it was not significantly correlated with the hippocampus.

The pre-SMA showed correlations with bilateral caudate and putamen, but was strongly anticorrelated with amygdala and hippocampus, as well as with parts of the VS and posterior putamen. However, this seed showed no significant correlation with SN.

Finally, the vmPFC was functionally correlated with bilateral VS, amygdala, and hippocampus, while anticorrelated with bilateral caudate and putamen. However, it was not significantly correlated with SN.

Seed-to-ROI Connectivity

Fisher z-transformed correlation coefficients were inputted in rmANOVAs for each of the 6 ROIs with the factor seed (Fig. 3 A); all *P*-values reported are stringently Bonferroni-corrected *P*-values.

The rmANOVAs showed significant differences between the 9 seeds in seed-to-VS, $F(6\,849) = 98.84$, $\eta^2_G = 0.35$, $P < 0.001$, seed-to-caudate, $F(7\,955) = 24.32$, $\eta^2_G = 0.11$, $P < 0.001$, and seed-to-putamen connectivity, $F(6\,890) = 68.26$, $\eta^2_G = 0.26$, $P < 0.001$. On post hoc analysis (Table 2), the bilateral dACC was more strongly correlated and the bilateral dmPFC more anticorrelated with the VS than any other seed explored, while both AI seeds and the bilateral vmPFC (with no differences between left and right AI, and bilateral vmPFC) showed stronger seed-to-VS correlations than dlPFC, IFC, and pre-SMA. In the case of connectivity to the caudate, however, post hoc *t*-tests revealed that the bilateral dmPFC was more functionally anticorrelated than any other seed (with no differences between dmPFC and vmPFC), while both bilateral dACC and pre-SMA were more positively correlated with the caudate than right AI, right dlPFC, right IFC, and bilateral vmPFC. There were further differences in seed-to-caudate connectivity between bilateral vmPFC and left AI and dlPFC. Finally, both AI seeds (with no differences between left and right AI) were more functionally correlated with the putamen than any of the other seeds; further significant differences existed between pre-SMA and both dmPFC and vmPFC, and between dmPFC and right IFC.

The rmANOVA further revealed significant differences between the 8 seeds (left and right AI, bilateral dACC, left and right dlPFC, right IFC, bilateral pre-SMA, bilateral vmPFC) in seed-to-amygdala connectivity, $F(5\,763) = 65.67$, $\eta^2_G = 0.25$, $P < 0.001$. On post hoc, this was driven by bilateral dlPFC, dACC, and pre-SMA (with no differences between these 4 seeds) being more strongly anticorrelated with the amygdala than bilateral AI, right IFC and vmPFC. Differences in seed-to-hippocampus connectivity were also evidenced by the rmANOVA performed on 6 seeds (bilateral dACC, left and right dlPFC, bilateral dmPFC, bilateral pre-SMA, bilateral vmPFC), $F(4\,626) = 108.48$, $\eta^2_G = 0.37$, $P < 0.001$. Post hoc testing showed that bilateral vmPFC was more positively correlated with this ROI than any other seed. Further, bilateral pre-SMA connectivity to the hippocampus was significantly more negative than for any other seed, except for bilateral dlPFC. The latter seeds were significantly more anticorrelated with the hippocampus than bilateral dACC, and there was a final significant difference between bilateral dmPFC and dACC.

The final rmANOVA revealed significant differences between the 6 seeds (left and right AI, bilateral dACC, left and right dlPFC, right IFC) in seed-to-SN connectivity, $F(4\,563) = 57.72$, $\eta^2_G = 0.19$, $P < 0.001$. On post hoc this was once again driven by both left and right AI being significantly more correlated with the SN than any other seed, with no differences between left and right AI, nor right AI and dACC. Further, the dlPFC, bilaterally, was more strongly anticorrelated with the SN than the right IFC, whereas bilateral dACC was more positively correlated with the SN than the dlPFC.

The differential patterns of connectivity of these seed-to-ROI analyses are summarized in Figure 3B.

Discussion

We report on functional connectivity of existing and emerging targets for noninvasive stimulation for disorders of addiction, comparing connectivity patterns to distal subcortical ROIs relevant to addictions in a sample of 145 healthy participants. Previous findings have demonstrated the link between invasive and noninvasive stimulation targets (Fox et al. 2014). Our results add to this body of work by providing evidence that cortical sites could be used to selectively target certain addiction-related subcortical regions based on their stronger connectivity, for instance stimulating dACC or AI to influence the VS or dlPFC to influence the amygdala. Our findings highlight possible mechanisms that might underlie efficacy of different cortical stimulation targets and further suggest that the selection of targets may be individualized based on known functional activity, connectivity patterns or cognitive endophenotypes.

Striatal Connectivity

The VS, and more specifically the NAcc, plays a central role in the pathophysiology of addiction (Everitt and Robbins 2005) and deep brain stimulation of this structure has been used successfully in small studies of treatment-refractory alcohol (Kuhn et al. 2007; Voges et al. 2013) and heroin dependence (Zhou et al. 2011; Kuhn et al. 2014), and has been incidentally found to reduce cigarette smoking (Kuhn et al. 2009; Mantione et al. 2010).

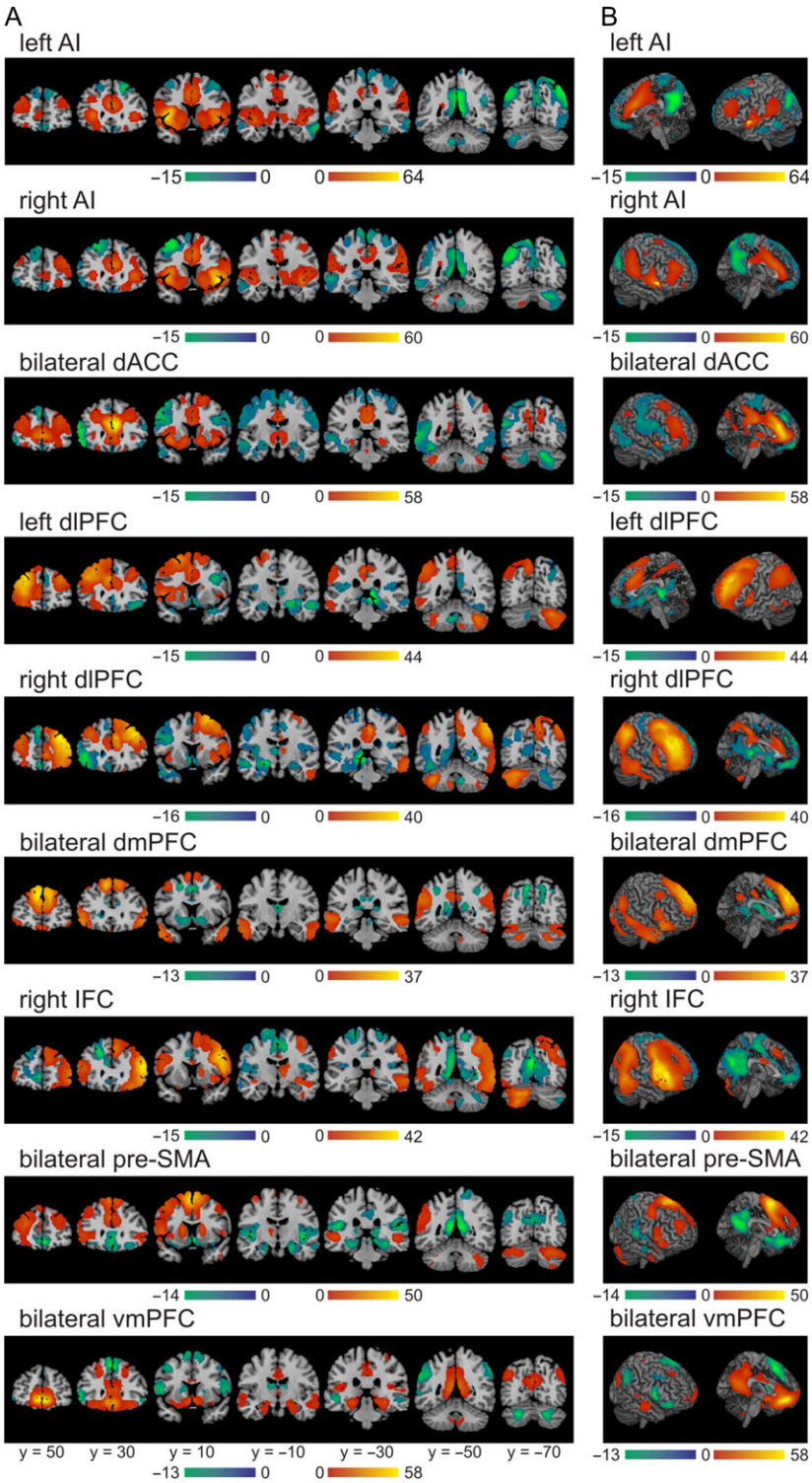

Figure 2. Seed-to-whole-brain resting-state functional connectivity of known and potential noninvasive stimulation targets. Results of the seed-to-whole brain resting-state functional connectivity in (*A*) representative slices and (*B*) cortex and midline. Images displayed at $P < 0.006$ (FWE-corrected) and $k > 0$.

In this study we show that, of the studied regions, bilateral AI appears to be most extensively connected with the striatum, with positive functional correlations with VS and putamen, making it a promising stimulation target. However, it should be taken into consideration that the deep stimulation needed to target the AI might also reach these subcortical structures (for an analysis of the induced fields during deep TMS, see Lu and Ueno 2017). We further show that bilateral dACC and vmPFC also are strongly correlated with the VS, suggesting they might be relevant if attempting to selectively target this distal region. However, the most commonly used target, the dlPFC, is mostly associated with the anterodorsal portion of the ipsilateral

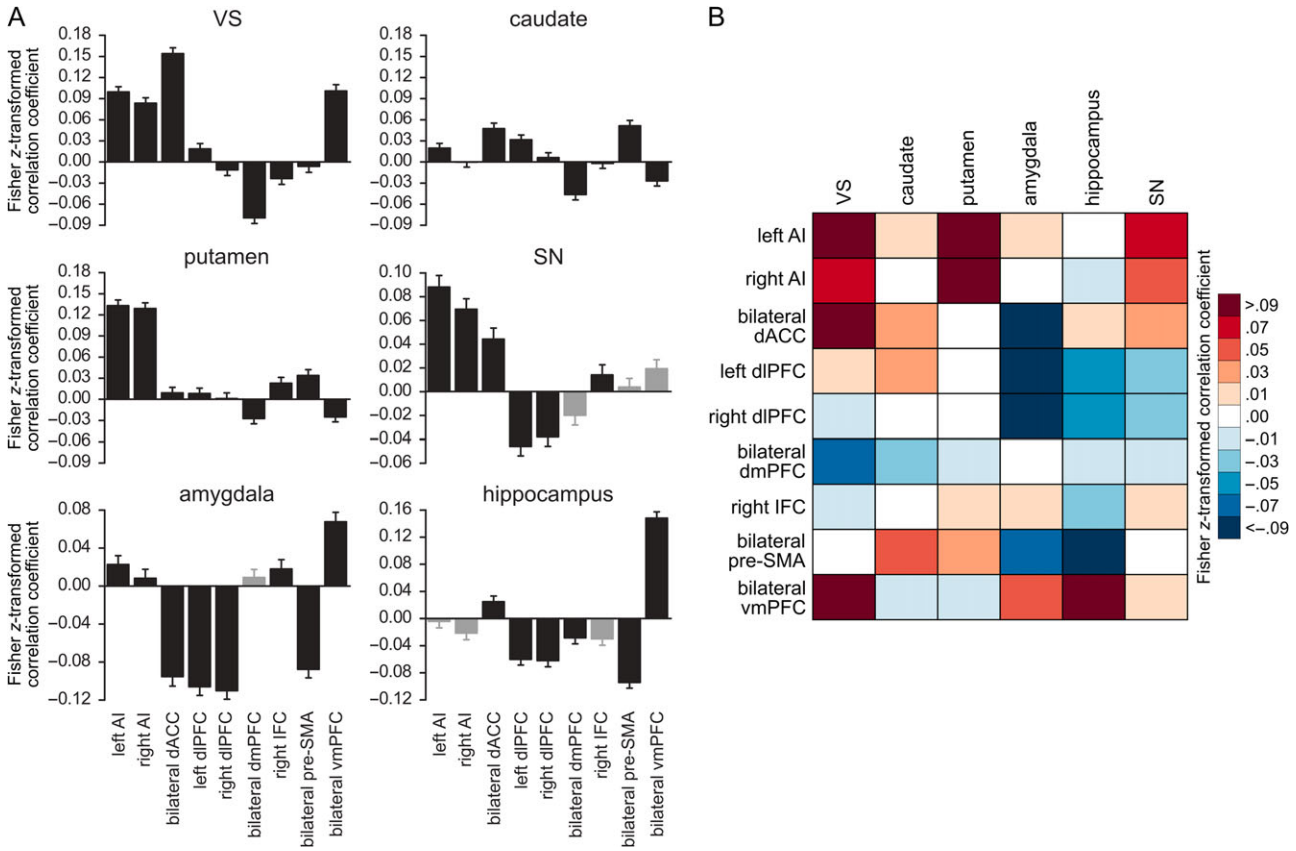

Figure 3. Seed-to-ROI analyses on resting-state functional connectivity of known and potential noninvasive stimulation targets. (*A*) Results of the post hoc tests on the seed-to-ROI analyses. Seeds that had demonstrated no statistically significant connectivity in the seed-to-whole brain analysis are represented with grey bars. Error bars represent the standard error of the mean. (*B*) Summary of the connectivity patterns revealed by the seed-to-ROI analyses. Red indicates correlation and blue anticorrelation; darker colors indicate stronger connectivity.

striatum, although in ROI analysis it does not appear to have markedly different striatal connectivity compared with other targets. In contrast, the dmPFC is predominantly characterized by negative connectivity with the VS, and less strongly with dorsal striatum, whereas the pre-SMA has mostly positive caudate connectivity.

These findings highlight potential target-dependent effects on cognitive function, and how stimulation frequency may be highly relevant (Nitsche and Paulus 2000; Post and Keck 2001). Indeed, previous studies have shown how low-frequency rTMS can result in an increase of the intrinsic correlations between multiple nodes within a resting-state network, with high-frequency rTMS showing the opposite effect (Vercammen et al. 2010; Eldaief et al. 2011). Our data suggest that attempts to influence VS function relevant to drug cue reactivity processes via cortical stimulation might yield very different results given whether these targets are positively (AI, dACC, vmPFC), negatively (dmPFC) or not considerably (right IFC, pre-SMA) correlated with the VS. Moreover, the currently favored dlPFC target (Mishra et al. 2010; Klauss et al. 2014) influences anterodorsal striatum and appears to have less strong connectivity to the VS than other cortical regions shown here, potentially explaining previous inconsistent stimulation results (Mishra et al. 2010; Höppner et al. 2011; Ceccanti et al. 2015; Terraneo et al. 2016). Our findings suggest that pre-SMA targeting may be more relevant when attempting to influence caudate-related functions such as goal-directed behaviors (Gläscher et al. 2010) or reactive inhibitory processes (Aron et al. 2007). In contrast, the AI and dmPFC may be relevant in attempts to influence putamen-related habitual behaviors, but notably with opposing direction of connectivity.

Within the studied targets, only AI, dACC and medial PFC seeds show strong functional connections to VS. It is particularly noteworthy that the dmPFC is anticorrelated with the VS, while dACC and vmPFC are positively correlated with this structure. Anatomical connectivity of the vmPFC and dACC in primates shows projections to subregions of the VS, with the focal projection field from the vmPFC concentrated within the NAcc, whereas the dmPFC projects to dorsomedial striatum and not VS (Haber and Knutson 2009). Our findings at rest are intriguing, but their functional relevance is not yet clear. The prelimbic PFC has been recently shown to exert suppressive control over reward-related signaling between dopaminergic midbrain and striatum in rats. Elevation of prelimbic PFC excitability led to suppression of striatal dopamine, inducing a decrease of reward-seeking behaviors (Ferenczi et al. 2016). Indeed, optogenetic stimulation of the prelimbic cortex prevents drug-seeking in cocaine-seeking rats (Chen, Yau, et al. 2013), although the exact homology of prelimbic rodent cortex with human PFC remains to be established. Altogether, these findings might open a new door for certain treatments, suggesting that the negative dmPFC–VS relationship seen in our resting-state data might also act as a potential target for noninvasive cortical stimulation. Moreover, the fact that adjacent regions within the medial PFC are both correlated and anticorrelated with the VS emphasizes the importance of selective

Table 2 Results of the pairwise comparisons performed on the average Fisher z-transformed correlation coefficients of the ROIs for the 9 seeds used in the resting-state functional connectivity analyses. Six ROIs were selected: VS, caudate, putamen, amygdala, hippocampus and SN. The 9 seeds used were left and right AI, bilateral dACC, left and right dlPFC, bilateral dmPFC, right IFC, bilateral pre-SMA and bilateral vmPFC. All *P*-values (significance threshold $P < 0.05$) are Bonferroni-corrected for 9 seeds, 6 ROIs and the number of pairwise comparisons performed ("–" denotes not performed comparisons)

ROI	Seed	Seed							
		Left AI	Right AI	Bilateral dACC	Left dlPFC	Right dlPFC	Bilateral dmPFC	Right IFC	Bilateral pre-SMA
VS	Right AI	n.s.							
	Bilateral dACC	<0.001	<0.001						
	Left dlPFC	<0.001	<0.001	<0.001					
	Right dlPFC	<0.001	<0.001	<0.001	n.s.				
	Bilateral dmPFC	<0.001	<0.001	<0.001	<0.001	<0.001			
	Right IFC	<0.001	<0.001	<0.001	ns	n.s.	<0.001		
	Bilateral pre-SMA	<0.001	<0.001	<0.001	n.s.	n.s.	<0.001	n.s.	
	Bilateral vmPFC	n.s.	n.s.	0.002	<0.001	<0.001	<0.001	<0.001	<0.001
Caudate	Right AI	n.s.							
	Bilateral dACC	n.s.	<0.001						
	Left dlPFC	n.s.	n.s.	n.s.					
	Right dlPFC	n.s.	n.s.	0.012	n.s.				
	Bilateral dmPFC	<0.001	0.037	<0.001	<0.001	<0.001			
	Right IFC	n.s.	n.s.	0.007	n.s.	n.s.	0.007		
	Bilateral pre-SMA	n.s.	0.002	n.s.	n.s.	0.011	<0.001	<0.001	
	Bilateral vmPFC	0.008	n.s.	<0.001	<0.001	n.s.	n.s.	n.s.	<0.001
Putamen	Right AI	n.s.							
	Bilateral dACC	<0.001	<0.001						
	Left dlPFC	<0.001	<0.001	n.s.					
	Right dlPFC	<0.001	<0.001	n.s.	n.s.				
	Bilateral dmPFC	<0.001	<0.001	n.s.	n.s.	n.s.			
	Right IFC	<0.001	<0.001	n.s.	n.s.	n.s.	0.011		
	Bilateral pre-SMA	<0.001	<0.001	n.s.	n.s.	n.s.	<0.001	n.s.	
	Bilateral vmPFC	<0.001	<0.001	n.s.	n.s.	n.s.	n.s.	n.s.	<0.001
Amygdala	Right AI	n.s.							
	bilateral dACC	<0.001	<0.001						
	Left dlPFC	<0.001	<0.001	n.s.					
	Right dlPFC	<0.001	<0.001	n.s.	n.s.				
	Bilateral dmPFC	–	–	–	–	–			
	Right IFC	n.s.	n.s.	<0.001	<0.001	<0.001	–		
	Bilateral pre-SMA	<0.001	<0.001	n.s.	n.s.	n.s.	–	<0.001	
	Bilateral vmPFC	n.s.	n.s.	<0.001	<0.001	<0.001	–	n.s.	<0.001
Hippocampus	Right AI	–							
	Bilateral dACC	–	–						
	Left dlPFC	–	–	<0.001					
	Right dlPFC	–	–	<0.001	n.s.				
	Bilateral dmPFC	–	–	0.018	n.s.	n.s.			
	Right IFC	–	–	–	–	–	–		
	Bilateral pre-SMA	–	–	<0.001	n.s.	n.s.	<0.001	–	
	Bilateral vmPFC	–	–	<0.001	<0.001	<0.001	<0.001	–	<0.001
SN	Right AI	n.s.							
	Bilateral dACC	0.013	n.s.						
	Left dlPFC	<0.001	<0.001	<0.001					
	Right dlPFC	<0.001	<0.001	<0.001	n.s.				
	Bilateral dmPFC	–	–	–	–				
	Right IFC	<0.001	<0.001	n.s.	0.001	<0.001	–		
	Bilateral pre-SMA	–	–	–	–	–	–	–	
	Bilateral vmPFC	–	–	–	–	–	–	–	–

stimulation, and shows how indirectly targeting the VS through noninvasive stimulation of the dACC might not be trivial.

Our findings also highlight the potential of the vmPFC as a stimulation target. The vmPFC is a critical node within the reward circuit (Haber and Knutson 2009) and the neurocircuitry of addiction (Everitt and Robbins 2005; Koob and Volkow 2010). White matter integrity between vmPFC and NAcc has been shown to be correlated with better reward learning performance (Samanez-Larkin et al. 2012), and tract strength between this region and striatum has shown to predict reward dependence (Cohen et al. 2009). Patients with lesions to the vmPFC have been reported to have decreased NAcc volumes, as well as reduced VS responses during reward anticipation (Pujara et al. 2016) and altered relative risk tolerance for prospective gains

and losses (Pujara et al. 2015). It has been suggested that the medial PFC controls the representation of contingencies, outcome values and subjective states associated to drugs, and that the transition from goal-directed to more habitual actions in drug-seeking might reflect a transition from PFC to striatal control (Everitt and Robbins 2005).

The direct anatomical AI to VS connection established in animal studies (Chikama et al. 1997; Schilman et al. 2008) has been demonstrated in humans by identifying projection tracts through the subcaudate white matter from AI to NAcc (Leong et al. 2016). Moreover, AI–VS connections have been linked to risk taking (Leong et al. 2016), reward anticipation and goal-directed action (Parkes et al. 2015), and suggested to modulate the transition between impulsive and compulsive behaviors (Weller et al. 2009; He et al. 2014; Belin-Rauscent et al. 2016). AI–NAcc tract coherence in humans is associated with lower impulsivity (Leong et al. 2016), whereas insula damage results in the impaired ability to adjust for expected values, leading to altered decision-making under risk (Weller et al. 2009). Indeed, the formation of maladaptive habits is key in the development of substance addiction (Everitt and Robbins 2005; Koob and Volkow 2010). Parkes et al. (2015) recently showed that AI–VS disconnection in rats leads to impaired outcome devaluation, resulting in the predominance of the habit over the goal-directed system. The AI and VS are also key nodes in the salience network relevant to drug cue reactivity.

We also show that the AI is the studied seed most strongly functionally correlated the SN. Midbrain dopaminergic regions play a key role in reinforcement processes (Berridge and Robinson 1998), which are crucial in the establishment and maintenance of addiction (Everitt and Robbins 2005; Koob and Volkow 2010). dlPFC shows negative connectivity with SN suggesting potential mechanisms that might underlie observations of enhanced striatal dopamine release with low-frequency rTMS of this region (Ko et al. 2008).

Amygdala and Hippocampal Connectivity

Amygdala and hippocampus are central nodes in drug craving (Koob and Volkow 2010). Both amygdala and hippocampus volumes have been found to be reduced in alcohol dependent subjects and binge drinkers (Makris et al. 2008; Howell et al. 2013; Mole et al. 2016), and heavy cannabis users (Schacht et al. 2012). Reduced amygdala, but not hippocampus, volumes have also been described in cocaine-dependent individuals (Makris et al. 2004). In resting-state, we demonstrate that dlPFC and pre-SMA show the strongest functional anticorrelations to both amygdala and hippocampus, whereas vmPFC shows the strongest correlation to both ROIs. In contrast, the dACC is strongly anticorrelated with the amygdala, but positively correlated with the hippocampus Indeed, a number of studies have reported decreased craving following high-frequency stimulation of the dlPFC (Camprodon et al. 2007; Politi et al. 2008; Mishra et al. 2010; Rapinesi et al. 2013; Girardi et al. 2015), which we suggest may be potentially mediated via an influence on distal mesial temporal regions. Further highlighting the importance of stimulation frequency, decreases in craving have been reported following low-frequency stimulation of the vmPFC (Hanlon et al. 2015).

The hippocampus is thought to play a central role in contextual conditioning in drug addiction (Everitt and Robbins 2005) and it has been shown that hippocampus-dependent memory formation is enhanced by reward-related activity (Wittmann et al. 2005). In rodents, hippocampus inactivation has been shown to suppress contextual reinstatement of cocaine-seeking behavior (Fuchs et al. 2005), whereas theta-burst stimulation of this structure reinstates extinguished cocaine-seeking behavior (Vorel et al. 2001).

The amygdala is particularly relevant to associative processes underlying the development of drug cues. Rodent studies have demonstrated that inactivation of different nuclei of the amygdala impairs the acquisition of drug-seeking behavior (Whitelaw et al. 1996), and prevents or attenuates alcohol cue-conditioned behavior (Millan et al. 2015). Further, selective lesions to the basolateral amygdala increase impulsive behavior (Winstanley et al. 2004). In both rodent and human studies, the amygdala has been implicated in memory reconsolidation, a process potentially relevant to therapeutic management of drug cues (Lee et al. 2006; Schwabe et al. 2014).

A recent study has found that the combination of low VS and high amygdala reactivity, as well as the opposite pattern, can predict problem drinking in young adults (Nikolova et al. 2016). Functional connectivity represents the level of linear association between 2 time series and, in particular, the interpretation of anticorrelations has been under debate (Fox et al. 2009), though it has been suggested that anticorrelated activity might relate to differential task-related responses in these structures (Greicius et al. 2003; Fox et al. 2005). How excitatory or inhibitory stimulation influences the direction of connectivity remains to be established. It has been shown that excitatory dlPFC stimulation enhances the negative connectivity between the central executive and the default mode networks, with inhibitory stimulation increasing the frequency range of the default mode network, suggesting its disinhibition (Chen, Oathes, et al. 2013). Further studies have shown similar patterns of high-frequency stimulation decreasing and low-frequency stimulation increasing connectivity patterns with other structures in networks observed at rest (van der Werf et al. 2010; Vercammen et al. 2010; Eldaief et al. 2011; Valchev et al. 2015). In the case of theta burst stimulation, it has been hypothesized that it might either inhibit the stimulated site and consequently disrupt the coactivation of further regions, or that the initial inhibition of the stimulation site might spread to other structures within the network (Mastropasqua et al. 2014). The work by Fox et al. (2014) strongly points to a link between positive and negative connectivity and efficacious noninvasive inhibitory and excitatory brain stimulation. Evidence suggests that, rather than just the local effect on the stimulated region, rTMS-induced changes in remote connectivity might underlie observed clinical outcomes (Grefkes et al. 2010; Vercammen et al. 2010; Fox, Buckner, et al. 2012; Philip et al. in press). Recent work has further highlighted the importance of network targeting in noninvasive stimulation, by demonstrating that multifocal tDCS substantially increased primary motor cortex excitability compared to tDCS targeting a single brain region (Fischer et al. 2017). Together with these studies, our observations with healthy subjects at rest suggest that specific cortical targeting depending on known cognitive endophenotypes might improve clinical outcomes, for example, by specifically targeting the VS with AI or dmPFC stimulation and the amygdala with dlPFC or pre-SMA stimulation.

Conclusion

In conclusion, we highlight differential patterns of subcortical functional connectivity depending on the cortical seed. We show the relevance of dACC and vmPFC as emerging cortical targets, and further emphasize the AI as a potential promising

target for noninvasive stimulation in the treatment of addiction, given its strong connections to VS, putamen, and SN. Our findings suggest that careful target selection based on known functional connectivity, consideration of direction of effect, along with the identification of cognitive endophenotypes to guide target selection might be crucial to therapeutic efficacy and may further lead to optimized personalized medicine approaches.

Supplementary Material

Supplementary material is available at *Cerebral Cortex* online.

Funding

Wellcome Trust as part of a Wellcome Trust Intermediate Fellowship to V.V. (983 705/Z/10/Z); Senior Clinical Fellowship of the Medical Research Council (MR/P008747/1 to V.V.); Research Fellowship of the Deutsche Forschungsgemeinschaft (DO1915/1-1 to N.D.).

Notes

Conflict of Interest: None declared.

References

Abdolahi A, Williams GC, Benesch CG, Wang HZ, Spitzer EM, Scott BE, Block RC, van Wijngaarden E. 2015. Smoking cessation behaviors three months following acute insular damage from stroke. Addict Behav. 51:24–30.

Aron AR, Durston S, Eagle DM, Logan GD, Stinear CM, Stuphorn V. 2007. Converging evidence for a fronto-basal-ganglia network for inhibitory control of action and cognition. J Neurosci. 27:11860–11864.

Baek K, Morris LS, Kundu P, Voon V. 2017. Disrupted resting-state brain network properties in obesity: decreased global and putaminal cortico-striatal network efficiency. Psychol Med. 47:585–496.

Belin-Rauscent A, Daniel ML, Puaud M, Jupp B, Sawiak SJ, Howett D, McKenzie C, Caprioli D, Besson M, Robbins TW, et al. 2016. From impulses to maladaptive actions: the insula is a neurobiological gate for the development of compulsive behavior. Mol Psychiatry. 21:491–499.

Berridge KC, Robinson TE. 1998. What is the role of dopamine in reward: hedonic impact, reward learning, or incentive salience? Brain Res Rev. 28:309–369.

Brett M, Anton J-L, Valabregue R, Poline J-B. 2002 Region of interest analysis using an SPM toolbox. Paper presented at the 8th International Conference on Functional Mapping of the Human Brain, Sendai, Japan.

Cai W, Cannistraci CJ, Gore JC, Leung H-C. 2014. Sensorimotor-independent prefrontal activity during response inhibition. Hum Brain Mapp. 35:2119–2136.

Cai W, George JS, Verbruggen F, Chambers CD, Aron AR. 2012. The role of the right presupplementary motor area in stopping action: two studies with event-related transcranial magnetic stimulation. J Neurophysiol. 108:380–389.

Cai W, Ryali S, Chen T, Li C-SR, Menon V. 2014. Dissociable roles of right inferior frontal cortex and anterior insula in inhibitory control: evidence from intrinsic and task-related functional parcellation, connectivity, and response profile analyses across multiple datasets. J Neurosci. 34:14652–14667.

Camprodon JA, Martínez-Raga J, Alonso-Alonso M, Shih M-C, Pascual-Leone A. 2007. One session of high frequency repetitive transcranial magnetic stimulation (rTMS) to the right prefrontal cortex transiently reduces cocaine craving. Drug Alcohol Depend. 86:91–94.

Ceccanti M, Inghilleri M, Attilia ML, Raccah R, Fiore M, Zangen A, Ceccanti M. 2015. Deep TMS on alcoholics: effects on cortisolemia and dopamine pathway modulation. A pilot study. Can J Physiol Pharmacol. 93:283–290.

Clewett D, Luo S, Hsu E, Ainslie G, Mather M, Monterosso J. 2014. Increased functional coupling between the left fronto-parietal network and anterior insula predicts steeper delay discounting in smokers. Hum Brain Mapp. 35:3774–3787.

Cohen MX, Schoene-Bake J-C, Elger CE, Weber B. 2009. Connectivity-based segregation of the human striatum predicts personality characteristics. Nat Neurosci. 12:32–34.

Cox SR, Ferguson KJ, Royle NA, Shenkin SD, MacPherson SE, MacLullich AMJ, Deary IJ, Wardlaw JM. 2014. A systematic review of brain frontal lobe parcellation techniques in magnetic resonance imaging. Brain Struct Funct. 219:1–22.

Chen AC, Oathes DJ, Chang C, Bradley T, Zhou Z-W, Williams LM, Glover GH, Deisseroth K, Etkin A. 2013. Causal interactions between fronto-parietal central executive and default-mode networks in humans. Proc Natl Acad Sci USA. 110:19944–19949.

Chen BT, Yau H-J, Hatch C, Kusumoto-Yoshida I, Cho SL, Hopf FW, Bonci A. 2013. Rescuing cocaine-induced prefrontal cortex hypoactivity prevents compulsive cocaine seeking. Nature. 496:359–362.

Chikama M, McFarland NR, Amaral DG, Haber SN. 1997. Insular cortical projections to functional regions of the striatum correlate with cortical cytoarchitectonic organization in the primate. J Neurosci. 17:9686–9705.

D'Urso G, Brunoni AR, Anastasia A, Micillo M, de Bartolomeis A, Mantovani A. 2016. Polarity-dependent effects of transcranial direct current stimulation in obsessive-compulsive disorder. Neurocase. 22:60–64.

da Silva MC, Conti CL, Klauss J, Alves LG, do Nascimento Cavalcante HM, Fregni F, Nitsche MA, Nakamura-Palacios EM. 2013. Behavioral effects of transcranial direct current stimulation (tDCS) induced dorsolateral prefrontal cortex plasticity in alcohol dependence. J Physiol Paris. 107:493–502.

De Ridder D, Vanneste S, Kovacs S, Sunaert S, Dom G. 2011. Transient alcohol craving suppression by rTMS of dorsal anterior cingulate: an fMRI and LORETA EEG study. Neurosci Lett. 496:5–10.

den Uyl TE, Gladwin TE, Wiers RW. 2015. Transcranial direct current stimulation, implicit alcohol associations and craving. Biol Psychol. 105:37–42.

Desikan RS, Ségonne F, Fischl B, Quinn BT, Dickerson BC, Blacker D, Buckner RL, Dale AM, Maguire RP, Hyman BT, et al. 2006. An automated labeling system for subdividing the human cerebral cortex on MRI scans into gyral based regions of interest. Neuroimage. 31:968–980.

Dinur-Klein L, Dannon P, Hadar A, Rosenberg O, Roth Y, Kotler M, Zangen A. 2014. Smoking cessation induced by deep repetitive transcranial magnetic stimulation of the prefrontal and insular cortices: a prospective, randomized controlled trial. Biol Psychiatry. 76:742–749.

Eichhammer P, Johann M, Kharraz A, Binder H, Pittrow D, Wodarz N, Hajak G. 2003. High-frequency repetitive transcranial magnetic stimulation decreases cigarette smoking. J Clin Psychiatry. 64:951–953.

Eldaief MC, Halko MA, Buckner RL, Pascual-Leone A. 2011. Transcranial magnetic stimulation modulates the brain's

intrinsic activity in a frequency-dependent manner. Proc Natl Acad Sci USA. 108:21229–21234.

Everitt BJ, Robbins TW. 2005. Neural systems of reinforcement for drug addiction: from actions to habits to compulsion. Nat Neurosci. 8:1481–1489.

Ferenczi EA, Zalocusky KA, Liston C, Grosenick L, Warden MR, Amatya D, Katovich K, Mehta H, Patenaude B, Ramakrishnan C, et al. 2016. Prefrontal cortical regulation of brainwide circuit dynamics and reward-related behavior. Science. 351.

Fischer DB, Fried PJ, Ruffini G, Ripolles O, Salvador R, Banus J, Ketchabaw WT, Santarnecchi E, Pascual-Leone A, Fox MD. 2017. Multifocal tDCS targeting the resting state motor network increases cortical excitability beyond traditional tDCS targeting unilateral motor cortex. Neuroimage. 157:34–44.

Fox MD, Buckner RL, Liu H, Chakravarty MM, Lozano AM, Pascual-Leone A. 2014. Resting-state networks link invasive and noninvasive brain stimulation across diverse psychiatric and neurological diseases. Proc Natl Acad Sci USA. 111: E4367–E4375.

Fox MD, Buckner RL, White MP, Greicius MD, Pascual-Leone A. 2012. Efficacy of transcranial magnetic stimulation targets for depression is related to intrinsic functional connectivity with the subgenual cingulate. Biol Psychiatry. 72:595–603.

Fox MD, Halko MA, Eldaief MC, Pascual-Leone A. 2012. Measuring and manipulating brain connectivity with resting state functional connectivity magnetic resonance imaging (fcMRI) and transcranial magnetic stimulation (TMS). Neuroimage. 62:2232–2243.

Fox MD, Snyder AZ, Vincent JL, Corbetta M, Van Essen DC, Raichle ME. 2005. The human brain is intrinsically organized into dynamic, anticorrelated functional networks. Proc Natl Acad Sci USA. 102:9673–9678.

Fox MD, Zhang D, Snyder AZ, Raichle ME. 2009. The global signal and observed anticorrelated resting state brain networks. J Neurophysiol. 101:3270–3283.

Fuchs RA, Evans KA, Ledford CC, Parker MP, Case JM, Mehta RH, See RE. 2005. The role of the dorsomedial prefrontal cortex, basolateral amygdala, and dorsal hippocampus in contextual reinstatement of cocaine seeking in rats. Neuropsychopharmacology. 30:296–309.

Girardi P, Rapinesi C, Chiarotti F, Kotzalidis GD, Piacentino D, Serata D, Del Casale A, Scatena P, Mascioli F, Raccah RN, et al. 2015. Add-on deep transcranial magnetic stimulation (dTMS) in patients with dysthymic disorder comorbid with alcohol use disorder: a comparison with standard treatment. World J Biol Psychiatry. 16:66–73.

Gläscher J, Daw ND, Dayan P, O'Doherty JP. 2010. States versus rewards: dissociable neural prediction error signals underlying model-based and model-free reinforcement learning. Neuron. 66:585–595.

Gorelick DA, Zangen A, George MS. 2014. Transcranial magnetic stimulation in the treatment of substance addiction. Ann N Y Acad Sci. 1327:79–93.

Gorini A, Lucchiari C, Russell-Edu W, Pravettoni G. 2014. Modulation of risky choices in recently abstinent dependent cocaine users: a transcranial direct-current stimulation (tDCS) study. Front Hum Neurosci. 8.

Grefkes C, Nowak DA, Wang LE, Dafotakis M, Eickhoff SB, Fink GR. 2010. Modulating cortical connectivity in stroke patients by rTMS assessed with fMRI and dynamic causal modeling. Neuroimage. 50:233–242.

Greicius MD, Krasnow B, Reiss AL, Menon V. 2003. Functional connectivity in the resting brain: a network analysis of the default mode hypothesis. Proc Natl Acad Sci USA. 100: 253–258.

Gu H, Salmeron BJ, Ross TJ, Geng X, Zhan W, Stein EA, Yang Y. 2010. Mesocorticolimbic circuits are impaired in chronic cocaine users as demonstrated by resting-state functional connectivity. Neuroimage. 53:593–601.

Haber SN, Knutson B. 2009. The reward circuit: linking primate anatomy and human imaging. Neuropsychopharmacology. 35:4–26.

Hanlon CA, Dowdle LT, Austelle CW, DeVries W, Mithoefer O, Badran BW, George MS. 2015. What goes up, can come down: novel brain stimulation paradigms may attenuate craving and craving-related neural circuitry in substance dependent individuals. Brain Res. 1628(Part A):199–209.

He Q, Xiao L, Xue G, Wong S, Ames SL, Schembre SM, Bechara A. 2014. Poor ability to resist tempting calorie rich food is linked to altered balance between neural systems involved in urge and self-control. Nutr J. 13:1–12.

Höppner J, Broese T, Wendler L, Berger C, Thome J. 2011. Repetitive transcranial magnetic stimulation (rTMS) for treatment of alcohol dependence. World J Biol Psychiatry. 12:57–62.

Howell NA, Worbe Y, Lange I, Tait R, Irvine M, Banca P, Harrison NA, Bullmore ET, Hutchison WD, Voon V. 2013. Increased ventral striatal volume in college-aged binge drinkers. PLoS One. 8:e74164.

Jacobson L, Javitt DC, Lavidor M. 2011. Activation of inhibition: diminishing impulsive behavior by direct current stimulation over the inferior frontal gyrus. J Cogn Neurosci. 23: 3380–3387.

Jacobson L, Koslowsky M, Lavidor M. 2012. tDCS polarity effects in motor and cognitive domains: a meta-analytical review. Exp Brain Res. 216:1–10.

Janes AC, Nickerson LD, Frederick BD, Kaufman MJ. 2012. Prefrontal and limbic resting state brain network functional connectivity differs between nicotine-dependent smokers and non-smoking controls. Drug Alcohol Depend. 125:252–259.

Johnson-Frey SH, Maloof FR, Newman-Norlund R, Farrer C, Inati S, Grafton ST. 2003. Actions or hand-object interactions? Human inferior frontal cortex and action observation. Neuron. 39:1053–1058.

Kim J-H, Lee J-M, Jo HJ, Kim SH, Lee JH, Kim ST, Seo SW, Cox RW, Na DL, Kim SI, et al. 2010. Defining functional SMA and pre-SMA subregions in human MFC using resting state fMRI: functional connectivity-based parcellation method. Neuroimage. 49:2375–2386.

Klauss J, Penido Pinheiro LC, Silva Merlo BL, Correia Santos GdA, Fregni F, Nitsche MA, Miyuki Nakamura-Palacios E. 2014. A randomized controlled trial of targeted prefrontal cortex modulation with tDCS in patients with alcohol dependence. Int J Neuropsychopharmacol. 17:1793–1803.

Ko JH, Monchi O, Ptito A, Bloomfield P, Houle S, Strafella AP. 2008. Theta burst stimulation-induced inhibition of dorsolateral prefrontal cortex reveals hemispheric asymmetry in striatal dopamine release during a set-shifting task—a TMS–[^{11}C]raclopride PET study. Eur J Neurosci 28:2147–2155

Koob GF, Volkow ND. 2010. Neurocircuitry of addiction. Neuropsychopharmacology. 35:217–238.

Kuhn J, Bauer R, Pohl S, Lenartz D, Huff W, Kim EH, Klosterkötter J, Sturm V. 2009. Observations on unaided smoking cessation after deep brain stimulation of the nucleus accumbens. Eur Addict Res. 15:196–201.

Kuhn J, Lenartz D, Huff W, Lee SH, Koulousakis A, Klosterkötter J, Sturm V. 2007. Remission of alcohol dependency following

deep brain stimulation of the nucleus accumbens: valuable therapeutic implications? J Neurol Neurosurg Psychiatry. 78: 1152–1153.

Kuhn J, Möller M, Treppmann JF, Bartsch C, Lenartz D, Gründler TOJ, Maarouf M, Brosig A, Barnikol UB, Klosterkötter J, et al. 2014. Deep brain stimulation of the nucleus accumbens and its usefulness in severe opioid addiction. Mol Psychiatry. 19: 145–146.

Kundu P, Inati SJ, Evans JW, Luh W-M, Bandettini PA. 2012. Differentiating BOLD and non-BOLD signals in fMRI time series using multi-echo EPI. Neuroimage. 60:1759–1770.

Lancaster JL, Woldorff MG, Parsons LM, Liotti M, Freitas CS, Rainey L, Kochunov PV, Nickerson D, Mikiten SA, Fox PT. 2000. Automated Talairach Atlas labels for functional brain mapping. Hum Brain Mapp. 10:120–131.

Lee JLC, Milton AL, Everitt BJ. 2006. Cue-induced cocaine seeking and relapse are reduced by disruption of drug memory reconsolidation. J Neurosci. 26:5881–5887.

Leong JK, Pestilli F, Wu Charlene C, Samanez-Larkin Gregory R, Knutson B. 2016. White-matter tract connecting anterior insula to nucleus accumbens correlates with reduced preference for positively skewed gambles. Neuron. 89:63–69.

Li X, Malcolm RJ, Huebner K, Hanlon CA, Taylor JJ, Brady KT, George MS, See RE. 2013. Low frequency repetitive transcranial magnetic stimulation of the left dorsolateral prefrontal cortex transiently increases cue-induced craving for methamphetamine: a preliminary study. Drug Alcohol Depend. 133:641–646.

Lu M, Ueno S. 2017. Comparison of the induced fields using different coil configurations during deep transcranial magnetic stimulation. PLoS One. 12:e0178422.

Ma N, Liu Y, Li N, Wang C-X, Zhang H, Jiang X-F, Xu H-S, Fu X-M, Hu X, Zhang D-R. 2010. Addiction related alteration in resting-state brain connectivity. Neuroimage. 49:738–744.

MacKillop J, Amlung MT, Acker J, Gray JC, Brown CL, Murphy JG, Ray LA, Sweet LH. 2014. The neuroeconomics of alcohol demand: an initial investigation of the neural correlates of alcohol cost-benefit decision making in heavy drinking men. Neuropsychopharmacology. 39:1988–1995.

Makris N, Gasic GP, Seidman LJ, Goldstein JM, Gastfriend DR, Elman I, Albaugh MD, Hodge SM, Ziegler DA, Sheahan FS, et al. 2004. Decreased absolute amygdala volume in cocaine addicts. Neuron. 44:729–740.

Makris N, Oscar-Berman M, Jaffin SK, Hodge SM, Kennedy DN, Caviness VS, Marinkovic K, Breiter HC, Gasic GP, Harris GJ. 2008. Decreased volume of the brain reward system in alcoholism. Biol Psychiatry. 64:192–202.

Mantione M, van de Brink W, Schuurman PR, Denys D. 2010. Smoking cessation and weight loss after chronic deep brain stimulation of the nucleus accumbens: therapeutic and research implications: case report. Neurosurgery. 66:E218.

Martinez D, Slifstein M, Broft A, Mawlawi O, Hwang D-R, Huang Y, Cooper T, Kegeles L, Zarahn E, Abi-Dargham A, et al. 2003. Imaging human mesolimbic dopamine transmission with positron emission tomography. Part II: Amphetamine-induced dopamine release in the functional subdivisions of the striatum. J Cereb Blood Flow Metab. 23:285–300.

Mastropasqua C, Bozzali M, Ponzo V, Giulietti G, Caltagirone C, Cercignani M, Koch G. 2014. Network based statistical analysis detects changes induced by continuous theta-burst stimulation on brain activity at rest. Front Psychiatry. 5:97.

Millan EZ, Reese RM, Grossman CD, Chaudhri N, Janak PH. 2015. Nucleus accumbens and posterior amygdala mediate cue-triggered alcohol seeking and suppress behavior during the omission of alcohol-predictive cues. Neuropsychopharmacology. 40:2555–2565.

Mishra BR, Nizamie SH, Das B, Praharaj SK. 2010. Efficacy of repetitive transcranial magnetic stimulation in alcohol dependence: a sham-controlled study. Addiction. 105: 49–55.

Mole TB, Mak E, Chien Y, Voon V. 2016. Dissociated accumbens and hippocampal structural abnormalities across obesity and alcohol dependence. Int J Neuropsychopharmacol. 19: 1–8.

Moran-Santa Maria MM, Hartwell KJ, Hanlon CA, Canterberry M, Lematty T, Owens M, Brady KT, George MS. 2015. Right anterior insula connectivity is important for cue-induced craving in nicotine-dependent smokers. Addict Biol. 20: 407–414.

Morris LS, Kundu P, Dowell N, Mechelmans DJ, Favre P, Irvine MA, Robbins TW, Daw ND, Bullmore ET, Harrison NA, et al. 2016. Fronto-striatal organization: defining functional and microstructural substrates of behavioural flexibility. Cortex. 74:118–133.

Murray GK, Corlett PR, Clark L, Pessiglione M, Blackwell AD, Honey GD, Jones PB, Bullmore ET, Robbins TW, Fletcher PC. 2007. Substantia nigra/ventral tegmental reward prediction error disruption in psychosis. Mol Psychiatry. 13: 267–276.

Nakamura-Palacios EM, Lopes IBC, Souza RA, Klauss J, Batista EK, Conti CL, Moscon JA, de Souza RSM. 2016. Ventral medial prefrontal cortex (vmPFC) as a target of the dorsolateral prefrontal modulation by transcranial direct current stimulation (tDCS) in drug addiction. J Neural Transm. 123: 1179–1194.

Naqvi NH, Rudrauf D, Damasio H, Bechara A. 2007. Damage to the insula disrupts addiction to cigarette smoking. Science. 315:531–534.

Nikolova YS, Knodt AR, Radtke SR, Hariri AR. 2016. Divergent responses of the amygdala and ventral striatum predict stress-related problem drinking in young adults: possible differential markers of affective and impulsive pathways of risk for alcohol use disorder. Mol Psychiatry. 21:348–356.

Nitsche MA, Paulus W. 2000. Excitability changes induced in the human motor cortex by weak transcranial direct current stimulation. J Physiol. 527:633–639.

Noda Y, Silverstein WK, Barr MS, Vila-Rodriguez F, Downar J, Rajji TK, Fitzgerald PB, Mulsant BH, Vigod SN, Daskalakis ZJ, et al. 2015. Neurobiological mechanisms of repetitive transcranial magnetic stimulation of the dorsolateral prefrontal cortex in depression: a systematic review. Psychol Med. 45: 3411–3432.

Öngür D, Ferry AT, Price JL. 2003. Architectonic subdivision of the human orbital and medial prefrontal cortex. J Comp Neurol. 460:425–449.

Parkes SL, Bradfield LA, Balleine BW. 2015. Interaction of insular cortex and ventral striatum mediates the effect of incentive memory on choice between goal-directed actions. J Neurosci. 35:6464–6471.

Philip NS, Barredo J, van't Wout-Frank M, Tyrka AR, Price LH, Carpenter LL. 2017. Network mechanisms of clinical response to transcranial magnetic stimulation in post-traumatic stress disorder and major depressive disorder. Biol Psychiatry. (in press).

Politi E, Fauci E, Santoro A, Smeraldi E. 2008. Daily sessions of transcranial magnetic stimulation to the left prefrontal cortex gradually reduce cocaine craving. Am J Addict. 17: 345–346.

Post A, Keck ME. 2001. Transcranial magnetic stimulation as a therapeutic tool in psychiatry: what do we know about the neurobiological mechanisms? J Psychiatr Res. 35:193–215.

Pujara MS, Philippi CL, Motzkin JC, Baskaya MK, Koenigs M. 2016. Ventromedial prefrontal cortex damage is associated with decreased ventral striatum volume and response to reward. J Neurosci. 36:5047–5054.

Pujara MS, Wolf RC, Baskaya MK, Koenigs M. 2015. Ventromedial prefrontal cortex damage alters relative risk tolerance for prospective gains and losses. Neuropsychologia. 79:70–75.

Rapinesi C, Kotzalidis GD, Serata D, Casale AD, Bersani FS, Solfanelli A, Scatena P, Raccah RN, Brugnoli R, Digiacomantonio V, et al. 2013. Efficacy of add-on deep transcranial magnetic stimulation in comorbid alcohol dependence and dysthymic disorder: three case reports. Prim Care Companion CNS Disord. 15:1–7.

Saiote C, Turi Z, Paulus W, Antal A. 2013. Combining functional magnetic resonance imaging with transcranial electrical stimulation. Front Hum Neurosci. 7:1–7.

Samanez-Larkin GR, Levens SM, Perry LM, Dougherty RF, Knutson B. 2012. Frontostriatal white matter integrity mediates adult age differences in probabilistic reward learning. J Neurosci. 32:5333–5337.

Sanches M, Caetano S, Nicoletti M, Monkul ES, Chen HH, Hatch JP, Yeh P-H, Mullis RL, Keshavan MS, Rajowska G, et al. 2009. An MRI-based approach for the measurement of the dorsolateral prefrontal cortex in humans. Psychiat Res-Neuroim. 173:150–154.

Schacht JP, Hutchison KE, Filbey FM. 2012. Associations between cannabinoid receptor-1 (*CNR1*) variation and hippocampus and amygdala volumes in heavy cannabis users. Neuropsychopharmacology. 37:2368–2376.

Schilman EA, Uylings HBM, Graaf YG-d, Joel D, Groenewegen HJ. 2008. The orbital cortex in rats topographically projects to central parts of the caudate–putamen complex. Neurosci Lett. 432:40–45.

Schwabe L, Nader K, Pruessner JC. 2014. Reconsolidation of human memory: brain mechanisms and clinical relevance. Biol Psychiatry. 76:274–280.

Senatorov VV, Damadzic R, Mann CL, Schwandt ML, George DT, Hommer DW, Heilig M, Momenan R. 2015. Reduced anterior insula, enlarged amygdala in alcoholism and associated depleted von Economo neurons. Brain. 138:69–79.

Sjoerds Z, Stufflebeam SM, Veltman DJ, Van den Brink W, Penninx BWJH, Douw L. 2017. Loss of brain graph network efficiency in alcohol dependence. Addict Biol. 22:523–534.

Skvortsova V, Palminteri S, Pessiglione M. 2014. Learning to minimize efforts versus maximizing rewards: computational principles and neural correlates. J Neurosci. 34: 15621–15630.

Terraneo A, Leggio L, Saladini M, Ermani M, Bonci A, Gallimberti L. 2016. Transcranial magnetic stimulation of dorsolateral prefrontal cortex reduces cocaine use: a pilot study. Eur Neuropsychopharmacol. 26:37–44.

Valchev N, určić-Blake B, Renken RJ, Avenanti A, Keysers C, Gazzola V, Maurits NM. 2015. cTBS delivered to the left somatosensory cortex changes its functional connectivity during rest. Neuroimage. 114:386–397.

van der Werf YD, Sanz-Arigita EJ, Menning S, van den Heuvel OA. 2010. Modulating spontaneous brain activity using repetitive transcranial magnetic stimulation. BMC Neurosci. 11:145.

Vercammen A, Knegtering H, Liemburg EJ, Boer JAd, Aleman A. 2010. Functional connectivity of the temporo-parietal region in schizophrenia: effects of rTMS treatment of auditory hallucinations. J Psychiatr Res. 44:725–731.

Voges J, Müller U, Bogerts B, Münte T, Heinze H-J. 2013. Deep brain stimulation surgery for alcohol addiction. World Neurosurg. 80:S28.e21–S28.e31.

Vorel SR, Liu X, Hayes RJ, Spector JA, Gardner EL. 2001. Relapse to cocaine-seeking after hippocampal theta burst stimulation. Science. 292:1175–1178.

Weller JA, Levin IP, Shiv B, Bechara A. 2009. The effects of insula damage on decision-making for risky gains and losses. Soc Neurosci. 4:347–358.

Whitelaw RB, Markou A, Robbins TW, Everitt Barry J. 1996. Excitotoxic lesions of the basolateral amygdala impair the acquisition of cocaine-seeking behaviour under a second-order schedule of reinforcement. Psychopharmacology (Berl). 127:213–224.

Whitfield-Gabrieli S, Nieto-Castañón A. 2012. *Conn*: a functional connectivity toolbox for correlated and anticorrelated brain networks. Brain Connect. 2:125–141.

Winstanley CA, Theobald DEH, Cardinal RN, Robbins TW. 2004. Contrasting roles of basolateral amygdala and orbitofrontal cortex in impulsive choice. J Neurosci. 24:4718–4722.

Wittmann BC, Schott BH, Guderian S, Frey JU, Heinze H-J, Düzel E. 2005. Reward-related fMRI activation of dopaminergic midbrain is associated with enhanced hippocampus-dependent long-term memory formation. Neuron. 45:459–467.

Zhou H, Xu J, Jiang J. 2011. Deep brain stimulation of nucleus accumbens on heroin-seeking behaviors: a case report. Biol Psychiatry. 69:e41–e42.